Applied Thermal Engineering 31 (2011) 1936–1942

Contents lists available at ScienceDirect

Applied Thermal Engineering

journal homepage: www.elsevier.com/locate/apthermeng

Solar powered vapor absorption system using propane and alkylated benzene AB300 oil

R.K. Al-Dadah [a,*], G. Jackson [b], Ahmed Rezk [a]

[a] School of Mechanical Engineering, University of Birmingham, Edgbaston, Birmingham B15-2TT, UK
[b] Petroleum Corporation of Jamaica, 36 Trafalgar Road, Kingston 10, Jamaica

ARTICLE INFO

Article history:
Received 3 June 2009
Accepted 27 February 2011
Available online 8 March 2011

Keywords:
Solar
Air conditioning
Absorption
Propane
Lubricating oils

ABSTRACT

This paper describes experimental work on a solar assisted vapour absorption air conditioning system using Propane (refrigerant) and Alkylated Benzene (AB300–refrigeration lubrication oil, absorbent). Preliminary experiments to assess the miscibility of propane in various lubricating oils namely Shell Clavus oils 32 and 64 and Alkylated Benzene oils AB150 and AB300 indicated that Propane is most miscible in Alkylated Benzene AB300. The vapour absorption system is a single stage absorption consisting of evaporator, absorber, generator and condenser. The system is equipped with heat pipes installed between the absorber and the pre-generator to recover the heat of absorption. The heat applied to the generator replicated the solar thermal energy based on the climatic conditions of Jamaica using flat plate collectors commonly used in Jamaica. Experiments at various evaporator, absorber and generator temperatures showed that the coefficient of performance of the system increases with increasing the generator temperature and with decreasing the absorber temperatures. The solar fraction for the flat plate collectors to produce the generator temperature needed to drive the absorption system is up to 50%.

1. Introduction

The invention of an absorption cooling cycle dates back to the 1700's followed by a series of development. In 1859 and 1950's it was the first use of water/ammonia and water/lithium bromide respectively [1]. Recently, the increase in electricity cost and environmental challenges have made heat-powered vapour absorption cooling systems more attractive for both residential and industrial applications [2], as the conventional air conditioning systems require high quality energy (electricity) generated from primary energy sources [3]. It was reported that the current energy systems based on fossil fuels are largely responsible among others for the present environmental and economic crisis. World energy demand and CO_2 emissions is expected to rise by some 60% by 2030 with respect to the beginning of this century [4]. Absorption chillers are widely utilised in the air-conditioning industry, in part because they can be activated by heat sources such as hot water (solar collectors), steam, and direct fired fossil fuels [5,6], instead of electricity and in part because of using environmentally friendly working fluids that satisfy both Montreal Protocol, 1988 and Kyoto Protocol, 1997 [7,8]. Absorption cooling systems can also be integrated with combined heat and power (CHP) systems to provide power, heating and cooling for applications such as the food and process industries [9–11]. This integration is known as Trigeneration and as Combined Heating Refrigeration and Power (CHRP). Also, the use of solar energy as a direct thermal energy source is of interest for many researchers, where there is a synchronisation between solar intensity and air conditioning load demand especially in tropical climates [12–14]. The aforementioned factors led to the belief that the solar driven cooling systems would become cost competitive with conventional cooling systems.

Current absorption cooling systems utilise two refrigerant/absorbent pairs; water/lithium bromide and ammonia/water. While the water/lithium bromide absorption system is commonly used for air conditioning applications, the ammonia/water system can be used for applications where temperatures lower than zero are needed. Water/Lithium bromide has the drawbacks of crystallisation at high concentration, corrosion to metals and is expensive [15]. The generator temperature needed for Water/Lithium Bromide is 90–120 °C and can only be met by compound parabolic collectors (CPC) and evacuated tube solar collectors which tend to have high capital cost [16]. The ammonia/water absorption system has the disadvantage of the great miscibility of ammonia and water,

* Corresponding author.
E-mail addresses: r.k.al-dadah@bham.ac.uk (R.K. Al-Dadah), Gary.Jackson@pcj.com (G. Jackson).

1359-4311/$ – see front matter © 2011 Elsevier Ltd. All rights reserved.
doi:10.1016/j.applthermaleng.2011.02.040

Nomenclature

c_p	Specific heat Capacity (kJ/kgK)
$\dot{m}$	Mass flow rate (kg/s)
P	Pressure (Bar)
Q	Heat transfer rate (kW)
s	Oil specific gravity
T	Temperature (C)
X	Refrigerant in oil mass fraction (%)
W	Power consumption of the pump (kW)

Greek letters

ρ	Density (kg/m^3)

Subscripts

a	absorber
crit	critical
e	evaporator
g	generator
in	inlet
l	liquid
man	manufacturer
o	oil
out	outlet
pg	pre-generator
r	refrigerant
sol	solution
w	water

which means large rectification columns are required to generate the ammonia, which adds to the complexity of the system and the high temperature demand of the generation process (125–170 °C). This high generator temperature demand makes it unsuitable for solar applications. Furthermore, ammonia is a toxic refrigerant and has the additional drawbacks of corrosiveness and explosiveness.

Research into alternative working pairs included using Trifluoroethane TFE (refrigerant)/N-methyle-2-pyrrolidone (NMP) absorbent [17], Propane (refrigerant)/Mineral oil (absorbent) [18] and Dimethylethylenurea (DMEU, absorbent)/R32, R125, R134a and R152a (refrigerants) [19]. The refrigerants used by Sawada et al. [17] and Jelinek et al. [19] are HFC refrigerants that have a high global warming potential. Propane on the other hand is a natural refrigerant that has zero ozone depletion potential and less than 3 global warming potential. However, the main disadvantage of propane is that it is classified as highly flammable class 3 refrigerant and the extent of system charge will be increased in an absorption system, leading to concerns over safety. Unlike most of flammable gases, propane has a narrow flammability range. Unless the propane/air mixture is between approximately 2.2 and 9.6% propane vapour, it can't burn. Moreover, propane can't ignite in the air unless there's an ignition source of 504 °C [20]. In addition, the safety issues can be accommodated by stringent rules regarding leak detection, electrical insulation and ventilation to move the propane concentration out of flammability range.

This paper presents an experimental investigation of a vapour absorption system using Propane and a lubricating oil. First the results of preliminary tests of the miscibility of Propane in four commonly used lubricating oils will be presented. This will be followed by a description of the experimental facility and the methodology used to evaluate the performance of the absorption system. The operating temperatures are important parameters that influence the absorption system, Table 1. The performance of the absorption system at various evaporator, generator and absorber temperatures will be presented. Finaly, the feasibility of obtaining the required hot water output from a solar flat plate collector in Jamaica tropical climate to drive the absorption system will be discussed.

2. Propane/lubricating oil miscibility

Preliminary experiments were conducted to examine the solubility of propane in various lubricating oils. Here the variation of the vapour pressure was taken as a measure of the degree of solubility. As the amount of refrigerant dissolved in the oil increases, its vapour pressure reduces and the difference between the vapour pressure of pure refrigerant and that of the refrigerant/oil mixture increases. The experiments were conducted in a Parr stirred reactor made of stainless steel type 316. The reactor is fitted with a 500 W electrical heating clamps connected to a rheostat for temperature control/variation and is thermally insulated to prevent heat loss to the environment. One thermocouple was fitted in the base of the unit to record solution temperature, and another thermocouple, at the top, for gas temperature. A pressure transducer and pressure relief valve were also connected. A motorised stirrer was used to ensure proper heat distribution and miscibility of components throughout the reactor for equilibrium measurements. The temperatures recorded for the thermocouples were within ±2.5% of the calibrated thermometers' readings; as per the manufacture's specification.

In the experiments, the dry weight of the equilibrium chamber was recorded. Then, 30 mL of mineral oil was injected and the weight was also recorded. The system was allowed to stand for 10 min to achieve thermal equilibrium. When the thermal equilibrium was achieved, the site glass of the chamber was marked at a level to achieve this same level for each run of the experiment. A refrigerant charging metre was then used to add to each 30 mL of oil, approximately 5, 10, 15, 20, 25 and 30 mL of R290. The different R290/mineral oil concentrations were mixed continuously with the motorised stirrer, maintaining the same thermal equilibrium. The equilibrium chamber and content was weighed for each run. In addition, the temperature and pressure readings were taken.

Fig. 1 shows the variation in the pressure difference between the mixture and that of pure propane with variation of the refrigerant charge added. Pure propane vapour pressure is obtained at the same temperature as that of the mixture and hence takes into account variation in the operating temperatures. It can be seen that

Table 1
The effect of operating conditions on absorption system performance.

Parameter	COP	Chiller Performance	Working fluids & References
T_e	Increases as T_e increases	Fixed T_c, T_a, T_g	Water Lithium bromide [7,24] Water Monomethylamine[26]
T_c	Decreases as T_c increases	Fixed T_e, T_a, T_g	Water Lithium bromide [7,24] Water Monomethylamine [26]
T_a	Decreases as T_a increases	Fixed T_e, T_c, T_g	Water Lithium bromide [7,27] Water Monomethylamine [26] Water Lithium iodide [27]
T_g	Increases as T_g increases	Fixed T_e, T_c, T_a	Water Lithium bromide [7,24,28] Water Lithium iodide [27]

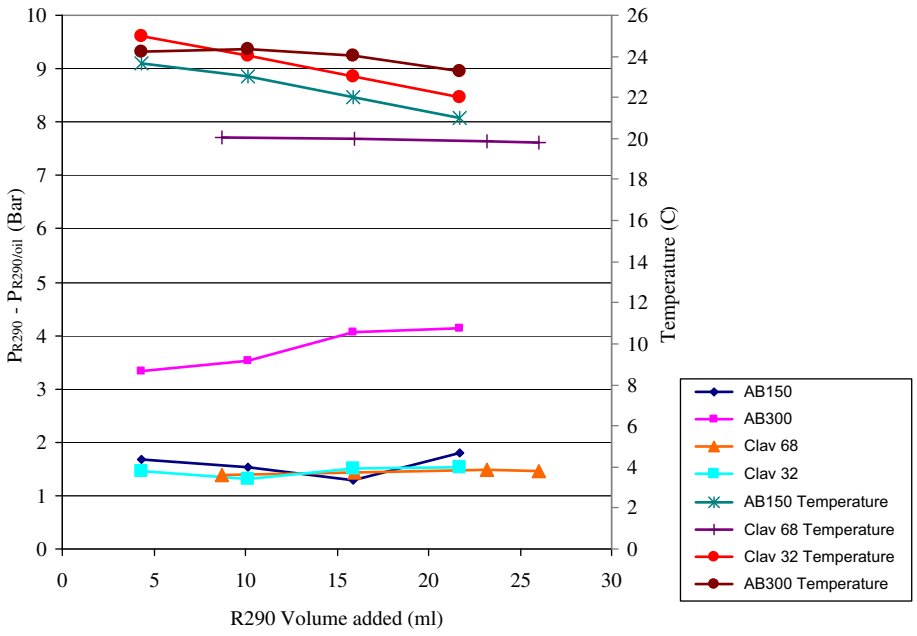

Fig. 1. Miscibility of Propane in various lubricating oils.

Alkylated Benzene AB300 produced the largest variation in pressure. This indicates that propane is more soluble in AB300 than any of the other oils tested. Hence it is used in the development of a vapour absorption system.

3. Vapour absorption system

Fig. 2 depicts a schematic diagram of a single stage absorption system fitted with absorber and generator. The condenser and evaporator are air cooled heat exchangers extracted from a split unit air conditioning system of 2.5 kW cooling capacity. The absorber and generator were specifically designed to fit with the air conditioning system. Here the generator was split into two parts, one part is installed above the absorber and the second part served as the main generator. The absorber was designed as a heat recovery vessel. It uses heat pipes to recover the heat of absorption. A bundle of fourteen heat pipes are arranged in a circular pattern as close as possible to enhance the heat recovery mechanism. The tubes are CRS series 5000 copper – water vapour heat pipes of 14 mm outside diameter and 619 mm length. The heat pipes were brazed to 150 mm brass plate. The section of the heat pipe above the brass plate is the condenser section where condensation occurs

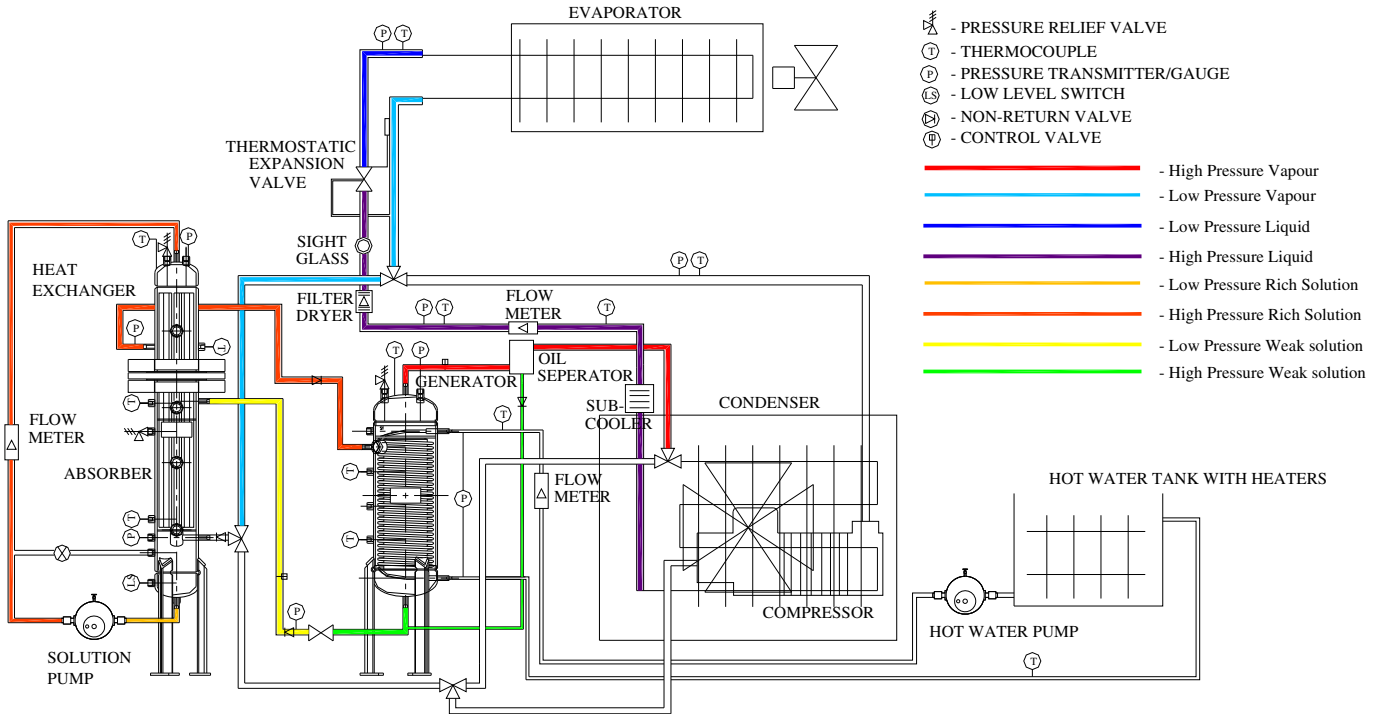

Fig. 2. Schematic diagram of the vapour absorption system.

and the section below the brass plate is the evaporator. At the top side of the brass plate, on the condenser side, is a 10 mm neoprene layer to reduce heat transfer between condenser and evaporator section of the heat pipe. The vessel surrounding the evaporator section of the heat pipes represents the absorber while that surrounding the condenser section of the heat pipes represent the pre-generator.

The absorber vessel has two inlets that were positioned to produce a counter flow between vapour and liquid. The lower of the two inlets introduces the low pressure vapour from the evaporator while the other (upper) inlet introduces the weak refrigerant in oil solution from the generator. Below the weak refrigerant in oil solution entry point of the absorber section, there is a perforated baffle plate with sleeve tubes. This will allow a homogeneous flow along the heat pipe in a thin laminar falling film. While the refrigerant vapour flows up, the falling oil film mixes with the vapour to form a stronger solution of refrigerant. The heat of absorption is absorbed by the evaporation of the heat pipe fluid and transported to preheat the strong refrigerant in oil solution in the pre-generator before flowing into the main generator. This solution is collected in a well inside the vessel where it floods the suction of the circulation pump. The pump pumps the strong refrigerant in oil solution from the absorber to the pre-generator. The pump increases the pressure from 3 bar absolute (operating pressure of the absorber) to 10 bar absolute (operating pressure of the generator). The absorber was fitted with four ¼" bulls-eye sight glasses that would allow the observation of the fluid mixture movement during the operation of the system. The absorber and pre-generator were fitted with five thermocouples to measure the temperature of the refrigerant vapour entering, the strong refrigerant in oil solution leaving and the weak refrigerant in oil solution entering the absorber and the solution entering and leaving the pre-generator.

The generator was designed to simulate the output conditions of a flat plate solar collector. The design operating temperature is 100 °C and the design pressure is 20 bar. The hot water heating coil in the generator is 6.25 mm copper coil with 28 turns on a 140 mm pitch circle diameter, to facilitate heat transfer along the length of the vessel. As the hot water flows through the coil, it heats the strong refrigerant solution and causes the generation of the refrigerant. The weak refrigerant in oil solution exits at the lower end of the generator, while the generated refrigerant vapour rises and exits at the top of the vessel. The hot water exits the generator and returns to the hot water tank. A circulating pump was connected in series to the tank to circulate the hot water through the generator. Customary solar collectors operate at a prescribed flow rate; hence, the experimental facility was fitted with a flow meter and a globe valve to control and measure the flow rate. To prevent excessive heat losses from the generator shell, a thermal insulation of *R*-value 3.90 m^2 kW^{-1} was used to insulate the body of the generator. Two thermocouples were installed at the hot water inlet and outlet to the generator. This allowed the measurement of the heat input to the generator. The evaporator was fitted in an air circulating duct where the air was heated and humidified before flowing over the evaporator. Thermocouples were inserted in various positions in the air-conditioning circuit, to assess the system performance.

The vessels and pipeline were instrumented with stainless steel pressure transmitters. There were two transmitters on the high/discharge pressure side pipe line and two on the low/suction pressure side for both vapour and liquid phases. They measure a pressure range of −1 to 40 bar gauge. The degree of accuracy as per manufacturer's specification is ≤0.2% of best fit straight line. The pipe lines and vessels have also been instrumented with K type thermocouples to measure the temperature of the refrigerant at the following points: the low pressure liquid, the low pressure vapour, the high pressure vapour and at the high pressure liquid before and after the sub-cooler. All the thermocouples were calibrated and their accuracy as per manufacturer specification is ±2.5%. The thermocouples were connected to a data logger and a personal computer was used to access the data from the data logger.

Three PLATON type flow metres were used in the system. The first one is to measure the refrigerant in oil solution pumped from the absorber to the pre-generator. The second flow meter was used to measure the refrigerant flow rate and was off the PLATON GU safety housed type with 0–1.2 l/min flow range. A sub-cooler was installed before the flow metre to ensure that the refrigerant reaches the flow metre in the liquid phase rather than a mixture allowing accurate reading of the flow rate. The third flow metre is used to measure the simulated hot water flow rate. The degree of accuracy of the flow metres is ±5% full scale deflection, with a repeatability of ±1% full scale deflection. A more detailed description of the experimental facility can be found in Jackson [21].

3.1. Vapour absorption system data analysis

The heat input to the generator is calculated from:

$$Q_g = \dot{m}_{gw} c_{pw} (T_{gwin} - T_{gwout}) \quad (1)$$

c_{pw} the specific heat capacity of water is taken as 4.187 kJ kg^{-1} K^{-1}. The heat pipes installed between the absorber and the pre-generator recover some of the heat of absorption process and transfer it to the pre-generator.

The rate of heat transferred from the absorber to the pre-generator was determined as:

$$Q_{pg} = \dot{m}_{pg} c_{psol} (T_{pgin} - T_{pgout}) \quad (2)$$

The refrigerant in oil mixture flow rate ($\dot{m}_{pg}$) was calculated using the measured volume flow rate and the density of the mixture. The density of the mixture was calculated using an equation proposed by Thome et al. [22] and given as:

$$\rho = \rho_0 / [1 - X_{aout} (\rho_0 / \rho_r - 1)] \quad (3)$$

$$\rho_0 = \rho_{man} [(T_{crit} - T)/(T_{crit} - (T_{man} + 273.15))]^{0.29} \quad (4)$$

Where ρ_{man} is the density of the oil as supplied by the manufacturer at specific temperature T_{man} (normally 15 °C), T_{crit} is the oil critical temperature (can be assumed to be 760 K for all oils as an approximation), T is the measured temperature (K). X_{aout} is the

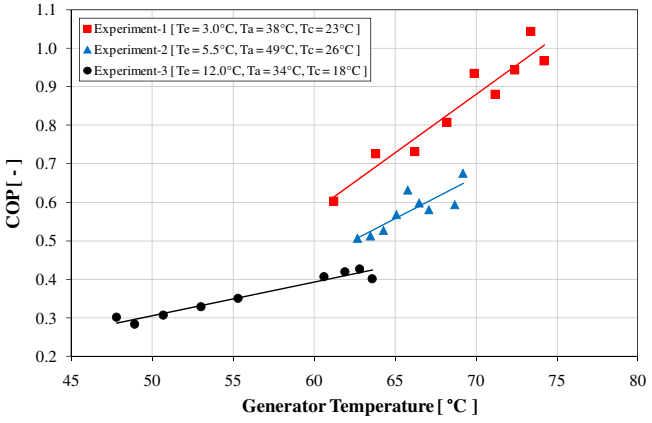

Fig. 3. The coefficient of performance versus generator temperature.

Table 2
Experimental COP in comparison with published data.

Experiment	COP	COP_{carnot}	T_e	T_a	T_c	T_g
Experiment-1	0.60	0.94	3	36	25	61
Experiment-2	0.51	0.69	5.6	46	26	63
Experiment-3	0.41	3.2	12	26	21	61
Keiceciler et al–1	0.39	0.98	3	40	20	60
Keiceciler et al–2	0.34	0.58	5.5	50	20	60
Florides et al	0.80	1.11	6	30	32	65

mass fraction of the refrigerant in oil solution at the exit of the absorber. The heat capacity of the refrigerant in oil solution (C_{psol}) was computed using equations (5)–(6) as recommended by Thome et al. [22].

$$c_{psol} = X_{aout}(c_{pL})_r + (1 - X_{aout})(c_{pL})_o \quad (5)$$

$$(c_{pL})_0 = 4.186\left\{[0.388 + 0.00045(1.8T + 32)]/s^{1/2}\right\} \quad (6)$$

Where s is the oil specific gravity as supplied by the manufacturer at $T = 15.56\ ^\circ C$.

The evaporator cooling load was calculated using the measured refrigerant volume flow rate and the refrigerant specific enthalpy difference across the evaporator. The refrigerant specific enthalpy values were obtained from state equations developed based on Propane published properties [23].

$$Q_{er} = \dot{m}_r(h_{erout} - h_{erin}) \quad (7)$$

The refrigerant mass flow rate ($\dot{m}_r$) was calculated from the measured volume flow rate and the density obtained at the measured temperature after the sub-cooler and the measured condenser pressure. The pump power was calculated using the measured input voltage and current.

$$W_p = 0.8 \times 1.732 \times V \times I \quad (8)$$

The constants 0.8 and 1.732 are to account for the load and three phase voltage.

The absorption system coefficient of performance (COP) was calculated using the evaporator cooling load and the rate of heat input to the generator and power required to drive the solution pump as:

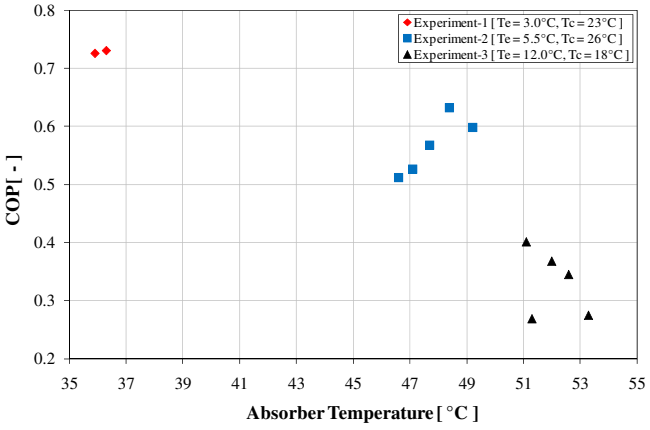

Fig. 4. Coefficient of performance versus absorber temperature at $T_g = 65\ ^\circ C$.

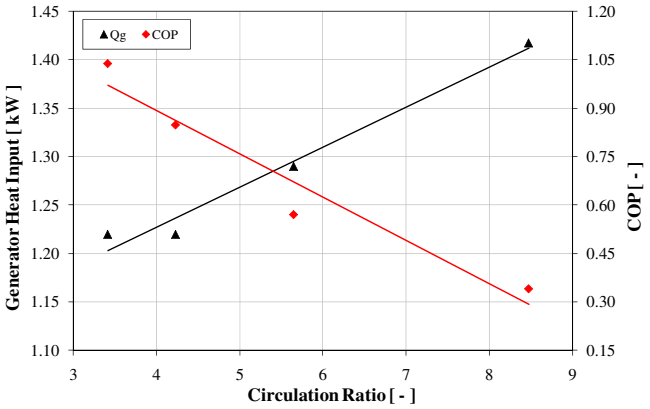

Fig. 5. The COP and generator heat input versus the circulation ratio.

$$COP = \frac{Q_{er}}{Q_g + W_p} \quad (9)$$

3.2. Results and discussion

Fig. 3 shows the variation of the COP with respect to the generator temperature for three different experiments at the evaporator, condenser and absorber temperatures listed in Table 2. It can be observed that the system COP increases as the generator temperature increases. Table 2 presents the average value of COP and the corresponding operating conditions in comparison of LiBr/Water absorption chillers of Keçeciler et al. [24] and Florides et al. [16]. Keçeciler et al. [24] used geothermal energy as the heat source to operate a single effect absorption system, while Florides et al. [16] used a solar compound parabolic collector. In all cases the generator outlet temperature was used. It can be seen that the average COP values produced by this experimental work is significantly higher than those produced by both Kececiler et al. [24] and Florides et al. [16]. Table 2 also shows the Carnot COP of the absorption system calculated by:

$$COP_{Carnot} = \frac{T_e(T_g - T_a)}{T_g(T_c - T_e)} \quad (10)$$

Equation 10 shows that the absorption system COP depends on the four working temperatures namely: evaporator temperature (T_e), generator temperature (T_g), absorber temperature (T_a) and condenser temperature (T_c) as depicted in Table 1. Fig. 4 shows the

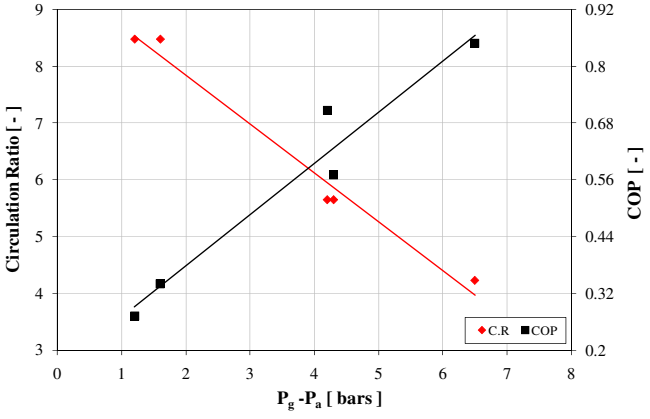

Fig. 6. Variation of the circulation ratio and the COP with the pressure difference between the generator and absorber.

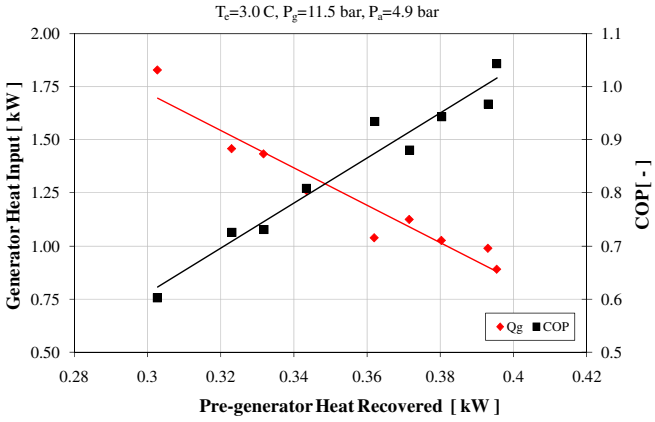

Fig. 7. Generator power input and COP versus the absorber heat exchanger heat gain.

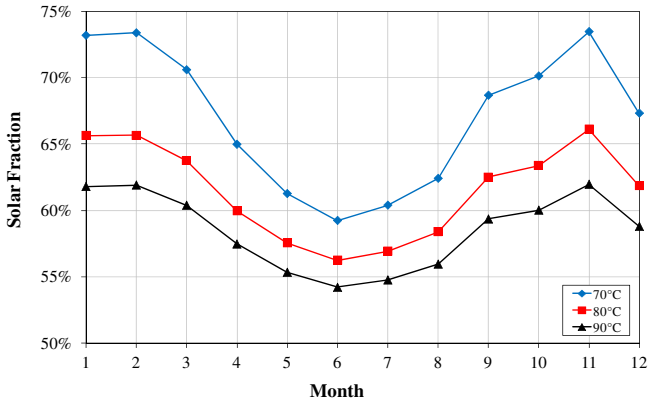

Fig. 9. Solar fraction monthly variation for producing hot water.

variation of the COP with the absorber outlet temperature at relatively constant generator outlet temperature of 65 °C and pressure for different evaporator temperatures where lower absorber outlet temperature resulted in higher COP.

Fig. 5 shows the variation of generator heat input and the COP with the circulation ratio. The circulation ratio is defined as the mass flow rate of the solution flowing out of the absorber to the mass flow rate of the refrigerant. It can be seen that the generator heat input increases with increasing the circulation ratio while the COP decreases. The circulation ratio increases by increasing the solution mass flow rate and/or decreasing the refrigerant flow rate. Decreasing the refrigerant flow rate results in reducing the cooling load and hence the COP while increasing the solution flow rate increases the required generator heat input and hence results also in reducing the COP. The variation of the circulation ratio with the pressure difference between the generator and absorber was plotted in Fig. 6. It can be seen that the circulation ratio decreases with increasing the pressure difference hence increasing the COP. This indicates that the rate of refrigerant generation increases with increasing the pressure difference thus increasing the cooling load and COP.

The presence of the heat pipes in the absorber/pre-generator provides heat recovery benefits to the system. The higher the amount of heat recovered, the lower the energy required from an external source to operate the system. Fig. 7 depicts the COP and the rate of heat supplied to the generator versus the rate of heat recovered by the heat pipes. It can be seen that as the rate of heat recovered by the heat pipes increases, the rate of heat required for the generator decreases and the coefficient of performance of the system increases. The rate of heat input required by the generator can be reduced by 40%.

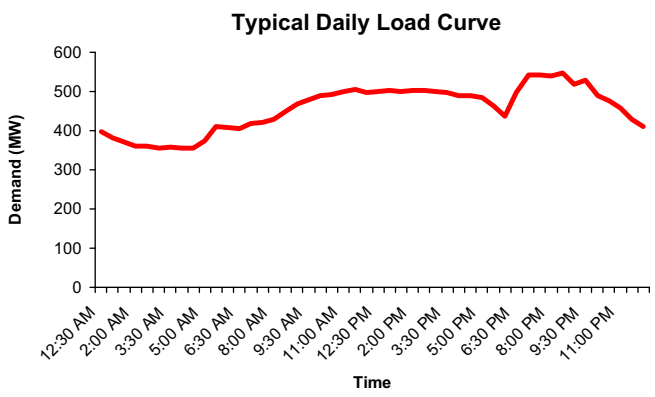

Fig. 8. Typical daily load demand profile of Jamaica.

4. Solar energy in Jamaica and air conditioning energy demand

The Caribbean region is located in the area between 10°N and 25°N and 85°W to 60°W, where the weather conditions in the summer season are classified as hot and humid with dry bulb temperatures as high as 40 °C. This hot and humid climate makes the cooling demand for domestic dwellings substantial. Fig. 8 gives a typical load profile of Jamaica. The load profile depicts a residential focus consumption pattern. The peak load occurs between 5:40 and 9:30 pm, an indication of extracting the high solar heat captured in a household during the day, using an air conditioning unit. Furthermore statistics of the power consumption in domestic houses in Jamaica indicate 40% of the energy consumption is associated with air conditioning systems [25]. Demand on cooling is also continuously increasing due to both increase in population and due to the increase in temperature due to global warming.

Most of the Caribbean countries use Flat Plate collectors to meet hot water demand. While less efficient than other solar collector types, its cost is less. This research aims to use the performance results of a flat plate collector to supply the thermal energy demand of the proposed absorption cooling system. The temperature of the hot water entering the generator in the above experiments ranged between 70 and 90 °C hot water. The average size of the common flat plate solar collector used in Jamaica has gross length 2.149 m, gross width 1.441 m, and gross depth 0.089 m. Fig. 9 shows the annual hot water production for a typical flat plate solar collectors system installed in Jamaica. To meet these temperatures, a combined solar flat plate collector and gas fired boiler is used. For such a system, the solar fraction defined by the percentage contribution of solar energy at set water temperature throughout the year was determined using software called Polysun4 (http://www.velasolaris.com/vs/component/option,com)_frontpage/Itemid,1/lang,en/. Fig. 9 shows the variation of the solar fraction at set temperatures of 70, 80 and 90. It can be seen that the solar fraction decreases with increasing the water output temperature. However, the solar fraction was above 50% in all months.

5. Conclusions

Propane miscibility tests using a “PARR instrument” in various lubricating oils concluded that Propane is most miscible in Alkylated Benzene AB300 as compared to AB150 and shell Clavus oils 32 and 64.

An absorption system utilising Propane and AB300 was constructed and its performance was evaluated at various generator, absorber and evaporator temperatures. The absorption system gave an effective cooling capacity of 1.3 kW. The COP increased with higher generator temperature. However, for the absorber, the system COP increases with decreasing the absorber temperature. A COP up to 1 was found, which was greater than the lithium bromide systems illustrated by Keçeciler et al. [24] and Florides et al. [16] at higher generator temperatures.

The absorption system using Propane and Alkylated Benzene AB300 can be driven by the hot water output of a flat plate collector operating under the weather conditions of Jamaica with solar fraction higher than 50%.

References

[1] P. Srikhirin, S. Aphornratana, S. Chungpaibulpatana, A review of absorption refrigeration technologies, Renewable and Sustainable Energy Reviews 5 (2001) 343–372.

[2] J.P. Praene, O. Marc, F. Lucas, Simulation and experimental investigation of solar absorption cooling system in Reunion Island, Applied Energy 88 (2011) 831–839.

[3] A.H.H. Ali, P. Noeres, C. Pollerberg, Performance assessment of an integrated free cooling and solar powered single-effect lithium bromide-water absorption chiller, Solar Energy 82 (2008) 1021–1030.

[4] P. Bermejo, F.J. Pino, F. Rosa, Solar absorption cooling plant in Seville, Solar Energy 84 (2010) 1503–1512.

[5] M. Izquierdo, R. Lizarte, J.D. Marcos, Air conditioning using an air-cooled single effect lithium bromide absorption chiller: results of a trial conducted in Madrid in August 2005, Applied Thermal Engineering 28 (2008) 1074–1081.

[6] A. Pongtornkulpanich, S. Thepa, M. Amornkitbamrung, Experience with fully operational solar-driven 10-ton LiBr/H2O single-effect absorption cooling system in Thailand, Renewable Energy 33 (2008) 943–949.

[7] B. Kim, J. Park, Dynamic simulation of a single-effect ammonia-water absorption chiller, International Journal of Refrigeration 30 (2007) 535–545.

[8] R.D. Misra, P.K. Sahoo, S. Sahoo, Thermoeconomic optimization of a single effect water/LiBr vapour absorption refrigeration system, International Journal of Refrigeration 26 (2003) 158–169.

[9] S.A. Tassou, D. Marriott, I. Chear, Trigeneration - A Solution to Efficient Use of Energy in the Food Industry. Institute of refrigeration, 2008.

[10] G.G. Maidment, G. Prosser, The use of CHP and absorption cooling in cold storage, Applied Thermal Engineering 20 (2000) 1059–1073.

[11] T.M. Mróz, Thermodynamic and economic performance of the LiBr–H2O single stage absorption water chiller, Applied Thermal Engineering 26 (2006) 2103–2109.

[12] O. Marc, J.-P. Praene, A. Bastide, Modeling and experimental validation of the solar loop for absorption solar cooling system using double-glazed collectors, Applied Thermal Engineering 31 (2011) 268–277.

[13] C. Monné, S. Alonso, F. Palacín, Monitoring and simulation of an existing solar powered absorption cooling system in Zaragoza (Spain), Applied Thermal Engineering 31 (2011) 28–35.

[14] T. Mateus, A.C. Oliveira, Energy and economic analysis of an integrated solar absorption cooling and heating system in different building types and climates, Applied Energy 86 (2009) 949–957.

[15] A.M. Al-Turki, M.M. Elsayed, Comparison of the solar-operated two-stage and single-stage LiBr–H2O absorption cycles, Solar & Wind Technology 7 (1990) 355–366.

[16] G.A. Florides, S.A. Kalogirou, S.A. Tassou, Modelling and simulation of an absorption solar cooling system for Cyprus, Solar Energy 72 (2002) 43–51.

[17] N. sawada, T. Tanaka, K. Mashimo, Development of organic working fluids and application to absorption systems, International Absorption and Heat Pump Conference (1993).

[18] M. Fukuta, T. Yanagisawa, H. Iwata, Performance of compression/absorption hybrid refrigeration cycle with propane/mineral oil combination, International Journal of Refrigeration 25 (2002) 907–915.

[19] M. Jelinek, A. Levy, I. Borde, The performance of a triple pressure level absorption cycle (TPLAC) with working fluids based on the absorbent DMEU and the refrigerants R22, R32, R124, R125, R134a and R152a, Applied Thermal Engineering 28 (2008) 1551–1555.

[20] K.L. Cashdollar, I.A. Zlochower, GM Green, Flammability of methane, propane, and hydrogen gases, Journal of Loss Prevention in the Process Industries 13 (2000) 327–340.

[21] G.C. Jackson, Solar Assisted Vapor Compression/absorption Air-condtioning System, in Mechanical Engineering. University of Birmingham, Birmingham, 2008.

[22] J.R. Thome, Engineering Data Book III. Wolvrine Tube Inc, 2004.

[23] ASHARE Handbook, Fundamental. ASHARE, 1999.

[24] A. Keçeciler, H.I. Acar, A. Dogan, Thermodynamic analysis of the absorption refrigeration system with geothermal energy: an experimental study, Energy Conversion and Management 41 (2000) 37–48.

[25] STATIN, Population Census. Living Arrangement, Vol. 5, Statistical institute of Jamaica, 2001.

[26] I. Pilatowsky, W. Rivera, R.J. Romero, Thermodynamic analysis of monomethylamine-water solutions in a single-stage solar absorption refrigeration cycle at low generator temperatures, Solar Energy Materials and Solar Cells 70 (2001) 287–300.

[27] K.R. Patil, S.K. Chaudhari, S.S. Katti, Thermodynamic design data for absorption heat transformers–part III. Operating on water-lithium iodide, Heat Recovery Systems and CHP 11 (1991) 361–369.

[28] U. Eicker, D. Pietruschka, Design and performance of solar powered absorption cooling systems in office buildings, Energy and Buildings 41 (2009) 81–91.